ACS OMEGA

http://pubs.acs.org/journal/acsodf

Article

Mesowestern Blot: Simultaneous Analysis of Hundreds of Submicroliter Lysates

Cameron O. Zadeh,[§] Jonah R. Huggins,[§] Deepraj Sarmah, Baylee C. Westbury, William R. Interiano, Micah C. Jordan, S. Ashley Phillips, William B. Dodd, Wesley O. Meredith, Nicholas J. Harold, Cemal Erdem, and Marc R. Birtwistle*

Cite This: *ACS Omega* 2022, 7, 28912−28923

Read Online

ACCESS | Metrics & More | Article Recommendations | Supporting Information

ABSTRACT: Western blotting is a widely used technique for molecular-weight-resolved analysis of proteins and their posttranslational modifications, but high-throughput implementations of the standard slab gel arrangement are scarce. The previously developed Microwestern requires a piezoelectric pipetting instrument, which is not available for many labs. Here, we report the Mesowestern blot, which uses a 3D-printable gel casting mold to enable high-throughput Western blotting without piezoelectric pipetting and is compatible with the standard sample preparation and small (∼1 μL) sample sizes. The main tradeoffs are reduced molecular weight resolution and higher sample-to-sample CV, making it suitable for qualitative screening applications. The casted polyacrylamide gel contains 336, ∼0.5 μL micropipette-loadable sample wells arranged within a standard microplate footprint. Polyacrylamide % can be altered to change molecular weight resolution profiles. Proof-of-concept experiments using both infrared-fluorescent molecular weight protein ladder and cell lysate (RIPA buffer) demonstrate that the protein loaded in Mesowestern gels is amenable to the standard Western blotting steps. The main difference between Mesowestern and traditional Western is that semidry horizontal instead of immersed vertical gel electrophoresis is used. The linear range of detection is at least 32-fold, and at least ∼500 attomols of β-actin can be detected (∼29 ng of total protein from mammalian cell lysates: ∼100−300 cells). Because the gel mold is 3D-printable, users with access to additive manufacturing cores have significant design freedom for custom layouts. We expect that the technique could be easily adopted by any typical cell and molecular biology laboratory already performing Western blots.

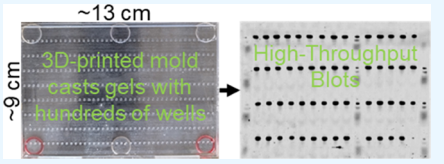

INTRODUCTION

The Western blot has been a staple of molecular biology research for decades since its first description in 1979.[1] It uses vertical immersed tank-based polyacrylamide gel electrophoresis (PAGE) to separate proteins by molecular weight, followed by transfer to a nitrocellulose or poly(vinylidene fluoride) (PVDF) membrane, and finally the application of antibodies to sensitively detect levels of proteins, posttranslational modifications, and even protein complexes.[2−4] Detection modalities include the enzyme-mediated generation of colorimetric molecules or light, or direct conjugation of fluorescent molecules to antibodies,[5,6] which, when combined with carefully designed experiments, can be quantitative.[7−9] Western blotting is still widely ingrained in biomedical research as a protein analytic tool, even perhaps the most used technique in protein-related publications in the last 10 years.[10] In fact, the use of Western blotting, despite falling "out of fashion", seems stable according to publication metrics.[10]

Although Western blot usage remains high, there are notable limitations. Reliance on antibodies for detection is increasingly criticized,[11,12] although the separation of proteins by molecular weight is a strong indicator of antibody validity not typically available to other antibody-based technologies, and Western blotting is often used as a confirmatory assay to bolster the support generated by other protein assays. Multiplexing is limited to a handful of analytes per gel, which can be increased slightly by stripping antibodies from the membrane and reprobing with new antibodies,[5,13] cutting the membrane into targeted molecular weight range strips for incubation of each with different antibodies,[14,15] or orthogonal detection methods.[16,17] Lastly, traditional Westerns are limited by throughput and sample size; typical gels contain only ∼10 wells for the analysis of 10 samples simultaneously, and each sample usually requires ∼10 ug of total protein content from cell or tissue lysates. It is this latter limitation of throughput and sample size that we focus on in this paper with the Mesowestern blot.

Before describing the Mesowestern blot, it is instructive to review the myriad of other related protein analytic technologies that address the shortcomings of the Western blot. Reverse-phase protein arrays (RPPAs) use lysates similar to Western

Received: April 8, 2022
Accepted: August 2, 2022
Published: August 11, 2022

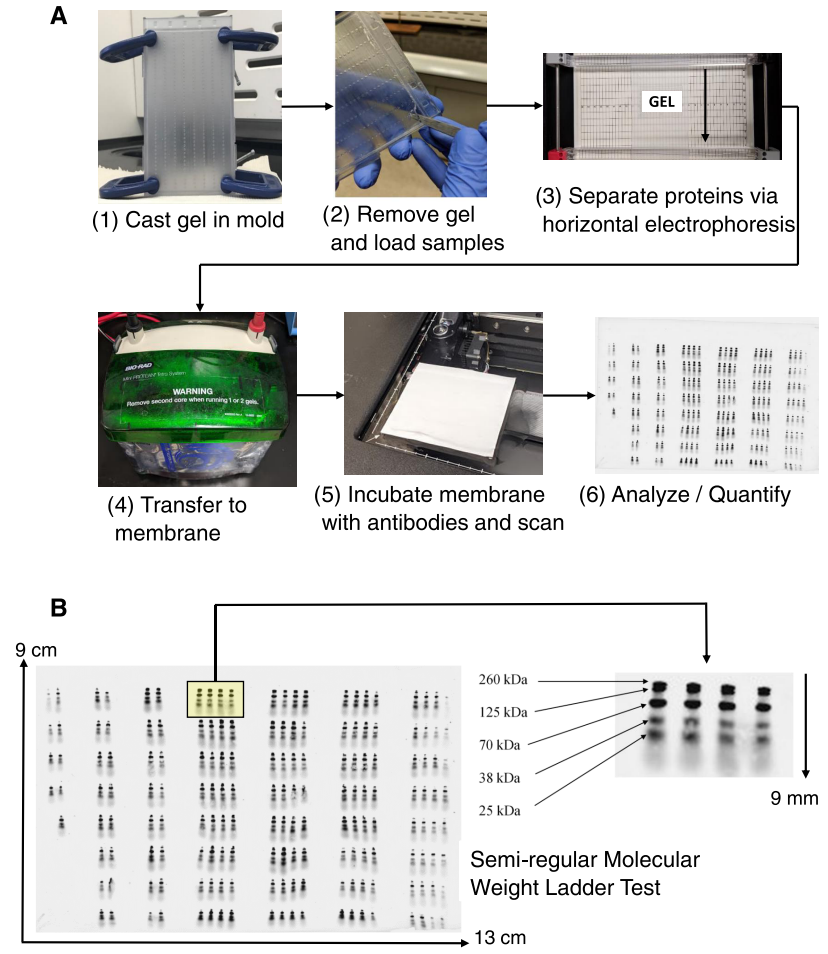

Figure 1. Mesowestern process and example results. A. First, the gel is polymerized in the gel casting mold, and after polymerization, it is removed so that samples can be loaded as desired. Electrophoresis takes place on a horizontal apparatus, which is the main difference between Mesowestern and regular Western. After electrophoresis, the Mesowestern and regular Western workflows are identical, with transfer to membrane (tank-based is shown), scanning/visualization, and analysis. B. An example Mesowestern PVDF membrane where the molecular weight ladder was loaded in semiregular patterns for illustrative purposes. The entire membrane scan is roughly of microplate dimensions, and one "block" of ladder is highlighted. A Mesowestern lane is only approximately 9 mm but resolves molecular weights between 125 and 25 kDa reasonably well (at 9.5% acrylamide used here). Electrophoresis was carried out at 100 V for ∼2 h.

blotting but greatly increase multiplexing by spotting lysates on chips so that hundreds of antibodies can be used simultaneously.[18,19] However, lysates are not separated by molecular weight, which causes increased stringency for antibody quality; in fact, antibodies are often validated for use in RPPA by Western blot. Luminex xMAP technology,[20] although technologically distinct from RPPA as it uses barcoded, antibody-conjugated beads, also offers increased multiplexing from cell lysates but does not separate proteins by molecular weight. Enzyme-linked immunosorbent assay (ELISA) has been established even longer than the Western blot and uses two antibodies, one to capture the analyte from a lysate and the other to detect the captured analyte, with detection modalities similar to Western blots.[21,22] Although ELISA does not separate analytes by molecular weight, the use of two different antibodies for the same target can, in some cases, compensate for specificity issues with one, although obviously the need for two antibodies can be a drawback itself. ELISA enables high-throughput implementation in multiwell plates for the simultaneous analysis of hundreds of samples. Mass spectrometry-based proteomics is antibody-free and can analyze virtually any protein present in a lysate so long as it is ionizable.[23−27] However, specific posttranslational modifications are not always observable.[5] Moreover, findings from mass spectrometry experiments often require orthogonal validation with antibody-based techniques such as a Western blot.[28] Thus, there remains space for a more high-throughput Western blot for analytes that are not amenable to mass spectrometry or when increased specificity is needed for antibodies. Moreover, Western blotting is likely to remain broadly useful as a complementary and confirmatory assay.

There have been advances in Western blotting itself that have improved on the aforementioned limitations. Single-cell Western blotting using PAGE (Protein Simple) has been developed, greatly reducing sample size requirements.[29,30] Other innovative Protein Simple apparati use capillary electrophoresis rather than a slab gel to allow analysis of up to 96 samples in a single loading (12 simultaneously) in a streamlined manner.[31−33] Digiwest combines Luminex technology with Western blotting by completing electrophoresis and transfer but then cutting the membrane into molecular weight sections to be analyzed by separate spectrally distinct beads.[34] This provides the multiplexing capabilities of Luminex with the molecular weight separation of Western. The

https://doi.org/10.1021/acsomega.2c02201
ACS Omega 2022, 7, 28912−28923

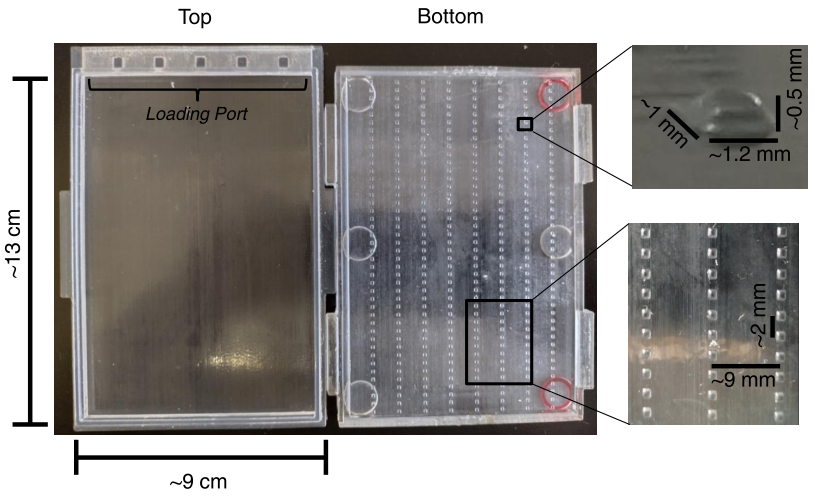

Figure 2. Gel casting mold. The mold consists of two pieces, which we refer to as "top" and "bottom". The top contains the loading port for the unpolymerized gel solution, whereas the bottom contains the raised regions, which become wells in the Mesowestern gel. The gel dimensions are approximately 9 cm by 13 cm in width and length and is 1.2 mm thick. Each well is a rectangle that is 1 mm by 1.2 mm in width and length and is 0.5 mm deep. Wells are spaced 1.8 mm apart and have 8.7 mm to run in their lane before the next well is reached.

Microwestern blot[35−37] uses a piezoelectric pipetting apparatus to spot nL amounts of lysate onto a typical-sized slab gel, followed by semidry horizontal electrophoresis (as opposed to tank-based), and finally, a gasket system for incubating different parts of the resultant membrane with up to 96 different antibodies. Thus, the Microwestern addresses both throughput and, to some extent, multiplexing limitations. However, the piezoelectric pipetting apparatus is not available to many labs.[35,37] There is not yet a slab gel-based Western technology that addresses throughput and sample size limitations that is micropipette-loadable.

Here, we present the Mesowestern blot that, similar to the Microwestern, allows for high-throughput analysis of hundreds of small samples in a typical-sized slab gel but does not require piezoelectric pipetting because it is micropipette-loadable. To do this, we designed and 3D-printed a gel casting mold that produces a polyacrylamide gel with 336, ~0.5 μL sample wells arranged with 8 rows by 42 columns in a microplate footprint. The main tradeoff is molecular weight resolution because samples have less distance to migrate. However, the format is flexible because the cast is 3D-printed and gel acrylamide % can be adjusted. Proof-of-concept experiments using both infrared-fluorescent molecular weight ladder and cell lysates demonstrate that proteins loaded in Mesowestern gels are amenable to the standard Western blotting steps of gel electrophoresis followed by the transfer to a membrane for imaging. These experiments also show another main tradeoff that sample-to-sample CV is high, making the technique more suited for qualitative screening applications. The main difference from Western blotting is horizontal electrophoresis as opposed to tank-based electrophoresis, and, as mentioned above, reduced molecular weight resolution. Because the gel mold is 3D-printable, users with access to institutional additive manufacturing cores (which are relatively commonplace) have significant design freedom for custom layouts. We expect that the technique could be easily adopted by any typical cell and molecular biology laboratory already performing Western blots.

RESULTS

Mesowestern Process. The Mesowestern process (Figure 1A) begins with casting a 1.2 mm thick polyacrylamide slab gel in the 3D-printed mold (Figure 2). The mold itself consists of two pieces, the "top" and "bottom". The top contains the ports in which the unpolymerized gel is loaded, and the bottom contains the impressions of the microwells into which lysates will be loaded after casting. Each microwell negative is roughly a trapezoidal prism (due to the nature of the 3D printer used) that is 0.5 mm in height and is slightly longer in the direction perpendicular to voltage (we found this results in better gel entry and less band dispersion compared to equal lengths or longer in the other direction). This gives a total volume of a little over 0.5 μL. The entire mold has dimensions of a microplate (~9 by 13 cm). It contains eight rows of microwell negatives, with each row containing 42 columns, for a total of 336 microwells per gel. Between rows, there is ~9 mm for proteins to separate and ~2 mm between microwells in the same row. All of these features are malleable by simply changing the CAD file for 3D printing.

During casting, the mold stands upright and is held tight by household C-clamps, while the freshly prepared unpolymerized gel solution (see the Methods section) is loaded into the casting device from the top, similar to traditional gel casting between glass plates. After polymerization (~30 min), the mold top and bottom are taken apart and the gel can be carefully removed for the loading of samples in the microwells via micropipette. After sample loading, horizontal electrophoresis separates proteins by molecular weight. This step is the biggest difference from the traditional Western blotting, which typically uses immersed tank vertical electrophoresis. Following electrophoresis, the workflow is generally indistinguishable from traditional Western blotting. Tank-based (or semidry) transfer can be employed to move the separated proteins to a nitrocellulose or PVDF membrane, membranes are incubated with antibodies (with block/wash steps), and finally scanned for the visualization of bands (we use LI-COR infrared fluorescence in this work).

As a simple demonstration, we loaded molecular weight ladder in semiregular patterns throughout a 9.5% acrylamide Mesowestern gel (Figure 1B). Although the distance each

https://doi.org/10.1021/acsomega.2c02201
ACS Omega 2022, 7, 28912−28923

sample has to run (~9 mm) is much smaller than the standard Western blot, and there is no "stacking gel" available, protein separation is reasonably uniform throughout the gel and molecular weight standards within the ladder are distinctly observable between 25 and ~125 kDa and to some extent at 260 kDa with lesser resolution. However, the tradeoff between Mesowestern and traditional Western—reduced molecular weight resolution—is clear. Overall, this pipeline establishes a Mesowestern workflow that is highly similar to traditional Western but is much higher throughput with smaller sample sizes.

Comparison of Macroscale Slab Western Technologies. After establishing the basic Mesowestern workflow, it is instructive to revisit the similarities and differences between that, the traditional Western, and the Microwestern,[36] the only other high-throughput slab Western technology (Figure 3 and

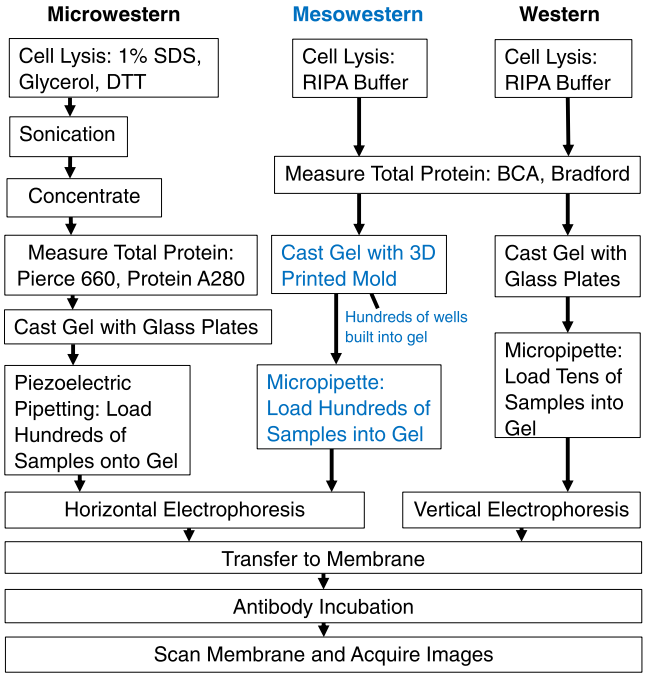

Figure 3. Comparison of Mesowestern to Microwestern and regular Western. There are significant differences between the Microwestern, the most comparable high-throughput slab Western, and the Mesowestern. In terms of processing and workflow, the Mesowestern is very similar to traditional Western. The main differences are that the gel is cast with the 3D-printed mold, rather than between two glass plates, that much smaller sample volumes are required, and that horizontal electrophoresis is employed. Horizontal electrophoresis is the main point of similarity between Microwestern and Mesowestern. The reliance of Microwestern on a piezoelectric pipetting apparatus creates several upstream problems, including the fact that there are no wells in a Microwestern gel, that lysis buffer is nonstandard and lysates must be sonicated and concentrated. After electrophoresis, the workflows of all three processes are the same.

Table 1). At the stage of sample preparation, Mesowestern and Western are identical, whereas Microwestern has multiple differences. Sodium dodecyl sulfate (SDS) and DTT are in the Microwestern lysis buffer, as opposed (primarily) to being added after lysis and during the preparation of samples to be loaded for Western and Mesowestern. This causes differences in the total protein content assays that can be used. In Microwestern, sonication steps to clear lysate (Covaris[36] or VialTweeter[37] as opposed to centrifugation) and spin column-based sample concentration[36,37] are used.

Both Microwestern and Western gels are cast with glass plates, whereas the Mesowestern uses the previously described 3D-printed mold. There are no wells in the Microwestern gel, whereas hundreds of small wells are built into the Mesowestern gel cast, and wells are introduced into a Western gel via a low polyacrylamide % stacking gel, which promotes subsequent sample focusing and improves band dispersion.[38] Also, gradient acrylamide % gels are available for Western,[39] but not for Microwestern or Mesowestern.

A primary difference with Microwestern is the piezoelectric pipetting-based "spotting" of samples, which then enter the well-less gel through adsorption or diffusion,[36] as compared to Mesowestern and Western where both use micropipettes to load samples into wells. The hundreds of Mesowestern gel wells hold ~0.5 μL of lysate each, whereas the ~10 Western gel wells hold ~10−40 μL of lysate each. During piezoelectric pipetting, ~10−20 μL of sample is needed in the microwell plate that serves as the sample source and also in the apparatus tubing to ensure robust spotting function.[37]

After samples are loaded, both the Microwestern and Mesowestern use semidry horizontal electrophoresis to separate proteins by molecular weight.[36,37] Western typically uses immersed tank-based vertical electrophoresis. After gel electrophoresis, there are a few differences between all three techniques with regard to transfer and preparation for antibody incubation/imaging. The Microwestern often uses a membrane gasket system to enable incubation with up to 96 different antibodies. The main differences also manifest with the molecular weight resolution, which is reduced for Microwestern and Mesowestern because there is no stacking gel and there is less distance for separation.

We conclude that the Mesowestern offers benefits compared to Microwestern, primarily the elimination of the reliance on piezoelectric pipetting. In comparison to the Western, the Mesowestern offers over 10-fold higher throughput with ~10-fold decreased sample volume requirements (we investigate sensitivity further below).

Controlling Molecular Weight Resolution by Varying Acrylamide Composition. Given the inherently lower-molecular-weight resolution of the Mesowestern as compared to that of the regular Western, we asked whether the acrylamide proportion could be varied in Mesowestern gels to enable more targeted separation of different molecular weight ranges. This is routinely done in regular Westerns. Therefore, we cast gels with 6, 9.5, 12, and 18% acrylamide compositions (see the Methods section) and evaluated the molecular weight separation of a ladder standard containing reference bands at 160, 90, 50, 30, and 15 kDa (Figures 4 and S1). Lower % gels should resolve higher-molecular-weight proteins more effectively and vice versa. Peaks in the corresponding intensity profiles corroborate visualized bands. We define a resolvable peak as a high point in line intensity profiles between two clearly identifiable troughs and dispersion as the trough-to-trough distance. Migration distance is the distance from the end of the well to the high point of a resolvable peak. To compare quantitatively across different gels, we focus on the 50 kDa band, which was resolvable in each (Table 2). In general, the migration distance and dispersion decrease as % acrylamide increases. In 6% gel, 160, 90, and 50 kDa standards are resolvable. In 9.5% gel, the 160, 90, 50, and 30 kDa standards are resolvable. The 50 kDa

https://doi.org/10.1021/acsomega.2c02201
ACS Omega 2022, 7, 28912−28923

Table 1. Comparison of Each Stage of the Western, Microwestern, and Mesowestern Methods

step	Microwestern array[35−37]	Mesowestern blot	Western blot
1. lysate preparation	∼20 μL per sample volume	∼1 μL per sample volume	∼10 μL per sample volume
	requires sonication	standard lysis buffers	standard lysis buffers
	requires high concentration (∼10 mg/mL), necessitating spin columns		
	nonstandard lysis buffers (e.g., contains SDS) dictate nonstandard protein concentration assays		
2. gel casting	uses glass plates to cast gels	uses 3D-printed mold to cast gels	uses glass plates to cast gels
	requires internal gel support structures (netfix)	hundreds of sample wells	tens of sample wells
	flat gel—no sample wells		stacking gel used
3. sample loading	hundreds of samples can be "spotted" with piezoelectric pipetting	hundreds of ∼1 μL samples can be loaded with micropipettes	tens of ∼10 μL samples can be loaded with micropipettes
4. protein separation	horizontal electrophoresis	horizontal electrophoresis	vertical (tank) electrophoresis
5. transfer	wet or semidry transfer	wet or semidry transfer	wet or semidry transfer
6. antibody incubation	incubate different sections or the entire membrane with antibodies	incubate different sections or the entire membrane with antibodies	incubate the entire membrane with antibodies.
7. analysis and quantification	lower-molecular-weight resolution due to smaller lanes	lower-molecular-weight resolution due to smaller lanes	distinct bands with greater-molecular-weight resolution due to larger lanes/stacking.

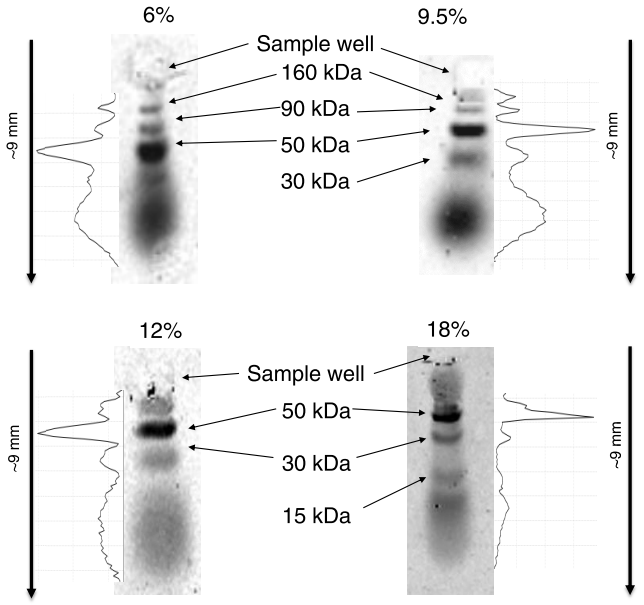

Figure 4. Acrylamide composition effects on molecular weight resolution. Representative examples from molecular weight ladder runs from four gels at different compositions of acrylamide (denoted by percent) are shown. Electrophoresis was carried out at 100 V for ∼2 h. Full scans are shown in Figure S1. Line intensity scans are overlaid for each image and were obtained from Image Studio (LI-COR). In general, as expected, higher acrylamide composition resolves lower molecular weights more robustly, at the expense of resolving higher molecular weights. When arrows are not shown, the peaks were not deemed resolvable.

band has lower dispersion in the 9.5% gel as compared to that in the 6% gel. In the 12% gel, the 50 and 30 kDa standards are resolvable. In the 18% gel, the 50, 30, and 15 kDa standards are resolvable. We conclude that varying acrylamide proportion in Mesowestern gels over ranges typically used in regular Western can resolve different molecular weight ranges, albeit with lower-molecular-weight resolution as compared to regular Western.

Reproducibility across a Mesowestern Gel. Having established the basic Mesowestern workflow using ladder-based standards, we wanted to evaluate the performance using

Table 2. Electrophoresis Metrics for the 50 kDa Marker in Gels with Varying Acrylamide Composition[a]

gel acrylamide (%)	migration distance (mm)	dispersion (mm)
6	2.7 ± 0.05	1.02 ± 0.02
9.5	1.97 ± 0.05	0.85 ± 0.03
12	1.58 ± 0.04	0.86 ± 0.03
18	1.06 ± 0.03	0.42 ± 0.02

[a]LI-COR Image Studio Lite was used to draw rectangular regions of interest around the band area of interest, and from line profiles, pixel lengths from the well to the peak (migration distance) or from peak trough to trough (dispersion) were measured in pixels. Conversion to mm was done using the imaging resolution of 84 um. Uncertainty is the standard error of the mean from 10 different lanes (full scans in Supporting Figure 1).

cell lysates and antibodies. The first question we had was related to the reproducibility across a gel. We specifically focused here on a "quarter gel", which we found often useful, as it still provides high-throughput capability but with reduced labor input. We loaded 0.5 μL of lysate from exponentially growing MCF10A cells into each well of a quarter gel, along with some regularly spaced molecular weight ladder, and then blotted for β-actin using LI-COR infrared fluorescence detection (Figure 5). The experiment yielded bands at the expected molecular weight (∼42 kDa), with a few anomalies not atypical from regular Western. There was a noticeable variability in the band intensities, which was found to follow a near-normal curve, with a CV of 33% (Figure 5B). Certainly, heterogeneities in electrophoresis and transfer to membrane could play a role, but we could also not rule out a substantial contribution from small volume manual pipetting. We conclude that the Mesowestern can be used to analyze cell lysates analogously to regular Western. Comparing values from direct quantification of bands in different parts of the membrane may be imprecise, and require normalization to additional controls. The high CV indicates that Mesowestern is best suited for qualitative screening applications at this stage.

Dual-Color Imaging Allows the Reduction of Variation by Normalization to a Loading Control. One feature of LI-COR-based infrared fluorescence approaches is a natural two-color imaging scheme, which in this case could provide an internal loading control signal for each well with which to

https://doi.org/10.1021/acsomega.2c02201
ACS Omega 2022, 7, 28912−28923

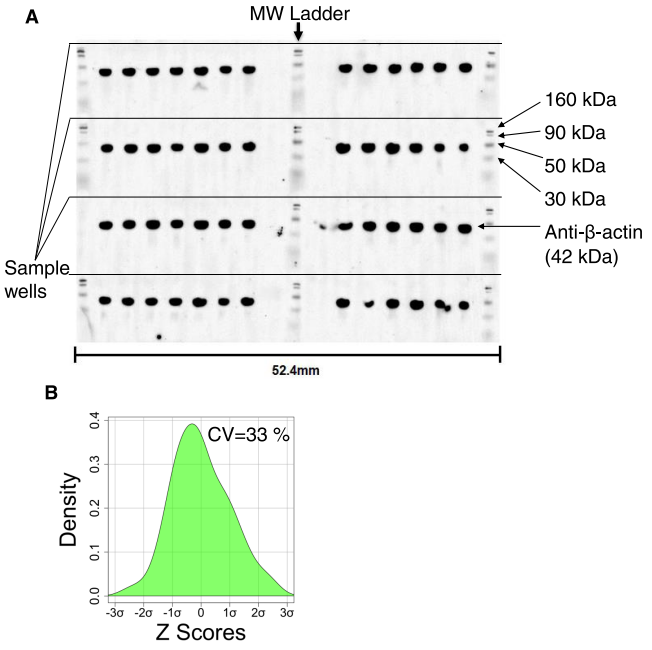

Figure 5. Lysates analyzed for reproducibility across a quarter gel. A. Exponentially growing MCF10A cells were harvested and lysed as described in the Methods section. The same lysate sample was loaded into each well of the pictured Mesowestern blot. The total protein concentration of the sample was 4.0 mg/mL, and 0.5 μL per well was loaded into the gel. After electrophoresis (100 V for ~2 h) and transfer, the PVDF membrane was incubated with anti-β-actin antibodies (1:1000) and a secondary antibody for detection (see the Methods section). B. We quantified each band (N = 52) in the blot image from A using Image Studio and analyzed the distribution by z-score analysis as pictured. The distribution is approximately normal, with very little variation outside of two standard deviations and a CV of 33%.

improve quantitative comparison from sample to sample. To test this, we again used a quarter gel loaded with cell lysates from exponentially growing MCF10A cells (Figure 6). As a loading control, we blotted for α-tubulin, and as an example of a target that may be of interest for quantification, we blotted for doubly phosphorylated ERK1/2 (p-MAPK), a central signal transduction protein. As before, bands were clearly visible at the expected molecular weights (Figure 6A,B). We note here that the individual ERK1 and ERK2 bands (42 and 44 kDa) are not resolvable by Mesowestern. We quantified the bands and found a reasonable correlation between their intensities (Figure 6C-R^2 = 0.69). To evaluate whether normalizing (i.e., dividing) the p-MAPK signal by the α-tubulin signal improved the reliability of the p-MAPK signal, we compared the CV for each set of values (Figure 6D). Such normalization reduced the CV for the p-MAPK signal, although it was still high at ~30% as above. We conclude that two-color imaging with internal loading controls may improve comparability across samples in a Mesowestern gel. However, as above, the high CV indicates that the Mesowestern at this point is best suited for qualitative screening applications.

Direct Comparison of Mesowestern and Western. We finally wanted to investigate sensitivity and linear range for Mesowestern in direct comparison to Western. While this will invariably be dependent on the epitope of interest, its abundance in the cell lysate, and the antibody being used, we started by investigating this for β-actin. Specifically, we performed a 6-point, 2-fold serial dilution of lysate from exponentially growing U87 cells and replicated this dilution curve 6 times on a portion of a Mesowestern gel (Figure 7A—we used a mold with slightly larger ~1 μL wells for this experiment; replicates in Figure S2). Simultaneously, 20 μL of the same lysates were loaded into a regular Western, and the same blocking and antibody solutions were used to compare Western to Mesowestern side by side (Figure 7B,C; replicates in Figure S2). Bands were observable from each technology in

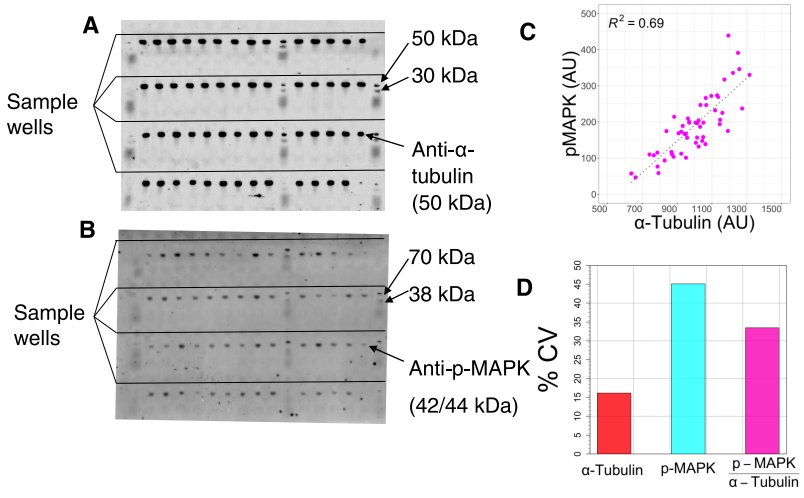

Figure 6. Dual-color Mesowestern blotting for loading control normalization. A–B. Lysate from exponentially growing MCF10A cells was diluted to 2 mg/mL and loaded into a 9.5% gel at 0.5 μL/well. After electrophoresis (100 V, ~2 h) and transfer, the PVDF membrane was incubated with anti-α-tubulin and anti-p-MAPK antibodies and then different secondary antibodies for the detection of each at different wavelengths. The membrane images depict the same membrane but at different wavelengths to detect A. α-tubulin and B. p-MAPK separately. C. Quantified bands (N = 55) were plotted to examine the expected correlation between the two signals from the same lysate. D. The variation across the gel of the independent signals and of the p-MAPK signal normalized by the α-tubulin loading control. Dividing by the loading control signal improves the % CV.

https://doi.org/10.1021/acsomega.2c02201
ACS Omega 2022, 7, 28912–28923

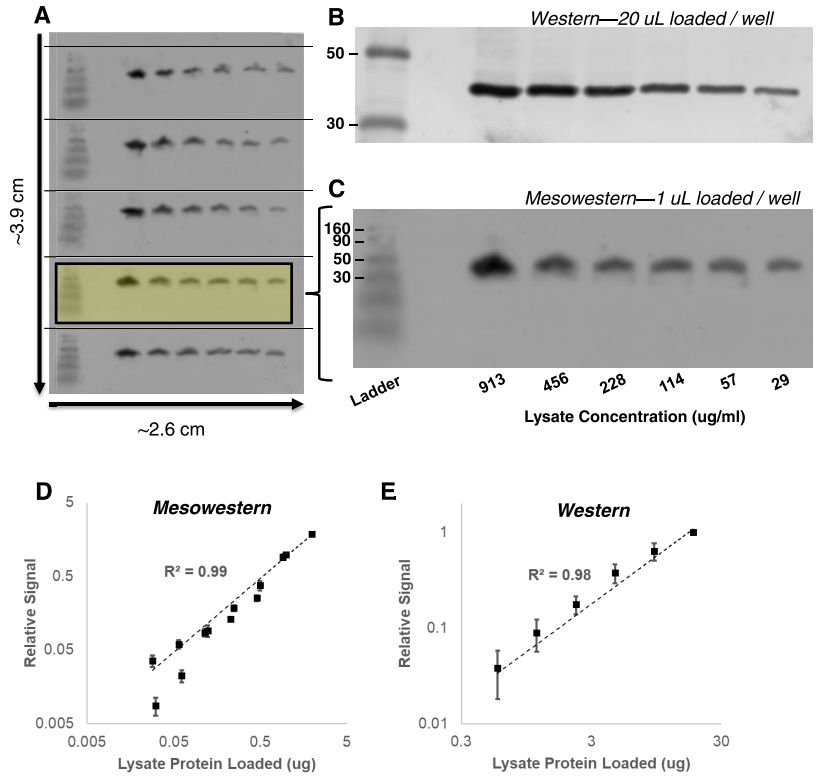

Figure 7. Comparison of Mesowestern and regular Western. A–C. Cell lysate from exponentially growing U87 cells was prepared at a range of protein concentrations (twofold serial dilution) and subjected to Mesowestern and Western analyses, as indicated. Full scans are shown in Figure S2. The PVDF membrane was incubated with anti-β-actin antibodies and a secondary antibody for detection. D, E. The signal derived from the image analysis of each band (N = 78 bands for Mesowestern from 2 blots and 14 dilution curves; N = 18 bands for Western from 3 blots/dilution curves) was plotted versus the known amount of total protein mass loaded. For Mesowestern (D), data were normalized such that 1 mg/mL lysate corresponds to a relative signal intensity of 1. For Western, data were normalized such that the maximum normalized signal was 1. Error bars are the standard error of the mean for each sample ($N \geq 3$).

each sample. We had expected the lowest concentration lysate to be below the limit of detection for Mesowestern, but to our surprise, this was not the case. In both cases, the linear range of detection was at least ~33-fold, with $R^2 \sim 0.99$ (Figure 7D). The lowest lysate concentration loaded in Mesowestern is at least equivalent to 29 ng of total protein, which is approximately 100–300 cells (0.1–0.3 ng of protein yield/cell).[40−42] Based on the estimates for absolute expression levels of β-actin in mammalian cells (~10^6 copies/cell),[43] this is at least ~500 attomol sensitivity, but as mentioned above, the serial dilution curve did not find the lower limit of detection. For regular Western, a 15 attomol limit of detection using the same infrared fluorescence modality has been reported for transferrin (no such data could be found for β-actin).[44] More broadly, the manufacturers report limits of detection for various modalities ranging from 500 fg to 500 pg of protein, which is consistent with ~10 attomol for proteins of typical molecular weight ranges.[45]

DISCUSSION

Here, we have described the development and first functional testing of a high-throughput, small sample size Western blotting protocol called Mesowestern. As compared to a Western blot, it enables at least 10-fold greater sample throughput with at least 1/10 the amount of lysate per sample and only requires horizontal as opposed to the traditionally employed vertical electrophoresis. The main tradeoff is the reduced molecular weight resolution because samples have a shorter separation distance and no stacking gel. Evaluation of sample-to-sample variability indicated that another limitation is the high CV, making this technique currently best suited for qualitative screening applications. As compared to the Microwestern, it eliminates the need for piezoelectric pipetting by using a 3D-printed gel mold that makes micropipette-loadable gels. We have demonstrated that the molecular weight resolution of a Mesowestern gel can be adjusted in expected ways by changing the gel acrylamide composition. We have explored the limits of detection and linear range of the Mesowestern, which was found to be largely similar to regular Western within the investigated ranges, although the lower limit of detection was not found with the given concentrations. Overall, the Mesowestern is a promising technology that could be readily adopted by molecular biology labs having interest in more high-throughput Western blotting with small sample sizes, particularly for qualitative screening applications.

Although we have used a single mold design here, the layout can be quite easily modified as users desire for their particular needs. Although most individual labs may not have the necessary 3D printing equipment, access to additive manufacturing facilities is relatively common and the printing itself is fast, so we anticipate that custom molds will be straightforward to implement. For example, some users may want fewer wells but to be able to load more sample volume per well. Others may want more separation space available to each well. Yet others may wish to make an even larger gel, much larger than a microwell plate footprint (compatible with

https://doi.org/10.1021/acsomega.2c02201
ACS Omega 2022, 7, 28912−28923

the downstream horizontal electrophoresis). All such variations are straightforward and possible depending on the needs that arise. Lastly, the commercial availability of gels could increase access.

One difference between the Mesowestern and regular Western is a "stacking" portion in a regular Western gel.[38,46] The stacking gel has a low acrylamide composition (~5%) with the purpose of allowing all of the proteins from the cell lysate to easily enter the subsequent "resolving" gel at the same time, which allows for decreased band dispersion and thus better molecular weight resolution. In the Mesowestern, there is only a resolving gel. In our applications so far, we indeed have noted that the resulting bands have higher dispersion than Western bands, although they were certainly identifiable at the expected molecular weight ranges. However, given the fact that Mesowestern inherently has lower-molecular-weight resolution due to less distance for proteins to migrate, future innovations incorporating stacking portions would be a welcome development. This is quite challenging, however, as the unpolymerized gel is loaded from a single entry port, making it difficult to isolate spatial regions where wells reside and stacking gels would be appropriate. In that regard, the ability to cast polyacrylamide gradient[39] Mesowestern gels would also be welcome but similarly challenging.

Lastly, although the Mesowestern makes significant advances with regard to throughput and sample size, we have not demonstrated here the multiplexing capabilities offered by Microwestern.[35,36] The Microwestern achieves high multiplexing (e.g., 96 antibody pairs at once) by placing the resultant membrane in a microwell plate-sized gasketing apparatus, which allows different antibodies on different parts of the membrane. There is no barrier to applying such an approach to the Mesowestern, so we expect that similar multiplexing can be done, albeit of course at the cost of being less high throughput, since wells must contain repeated patterns of the same lysates to be then blotted by different antibodies.

In conclusion, we have demonstrated here a new approach to Western blotting called the Mesowestern that increases throughput greater than 10-fold with greatly reduced sample size requirements. Given the tradeoffs of molecular weight resolution and sample-to-sample CV, qualitative screening applications are likely most suitable. Most notably, the Mesowestern is straightforward to implement in typical cell and molecular biology labs having a few dissimilarities from Western blotting. While the Western blot may be viewed by some as "old" and "irrelevant", it does in fact remain as one of the most widely used assays in biomedical science,[10] and this is unlikely to change due to its popular use as a sensitive and specific confirmatory assay modality. Thus, improvements to Western such as the Mesowestern we developed here are still expected to have a widespread impact.

METHODS

Printing the Mold. Molds were printed in the Clemson Additive Manufacturing Lab with the Stratasys Connex 350 and Veroclear as the material (Stratasys, OBJ-03271-RGD810). Following printing, a self-forming valve packing (Danco, #80794) was inlayed into the outer edge of the well perforation unit (bottom). Schematic files are available upon collaborative request.

Casting a Gel. Gel casting was completed through a process of silanization of surfaces coming into contact with the gel, clamping to ensure a tight leak-proof fit, and serological pipetting of unpolymerized solution into the mold. Briefly, a 2.5% v/v silane solution was prepared by combining 1.25 mL of dichlorodimethylsilane (Sigma-Aldrich, #40140) and 48.75 mL of 100% ethanol (Fisher, #04-355-22) in a 50 mL conical tube (Fisher, 14-432-22). We then applied 250 μL of the silane solution to the interior surfaces of both the top and bottom mold pieces, gently spread it across the surface by rocking, and wicked excess with a kimwipe. After assembling the top and bottom pieces together, four C-clamps (Irwin #1901235) were tightened onto the assembly at the designated corner locations (indented circles). At this point, the assembly is ready for loading.

A 9.5% gel solution was prepared by combining 47.5 mL of 30% bis/acrylamide solution 29:1 (BIO-RAD, #161-0156) with 41 mL of MilliQ water, 30 mL of glycerol (Sigma-Aldrich, #G5516-500 mL), 30 mL of 5× tris-acetate buffer (recipe as follows), and 1.5 mL of 10% sodium dodecyl sulfate (SDS) (Fisher, #BP 2436) together. Preparation of the 5× tris-acetate buffer was completed by dissolving 145.4 g of tris base (BIO-RAD, 161-0719) in 700 mL of MilliQ water (pH expected between 11.0 and 11.4). The pH was adjusted by adding 65 mL of glacial acetic acid (Sigma-Aldrich, #320099) and allowing the solution to sit overnight. Then, 0.5 mL of glacial acetic acid was pipetted into the solution and allowed to sit for an hour at room temperature. This was repeated until the solution reached pH 6.9. Finally, the volume of the solution was brought up to 1 L with MilliQ water and stored at 4 °C.

Polymerizing gel solution was made by combining 15 mL of 9.5% gel solution with 133 μL of 10% ammonium persulfate solution (APS) and 13.3 μL of TEMED (BIO-RAD #161-0700) into a beaker under a fume hood. The 10% APS solution was prepared by dissolving 0.2 g of ammonium persulfate (BIO-RAD #161-0800) into 2 mL of MilliQ water. Quickly after preparation, 15 mL of gel solution was dispensed by serological pipetting into the mold assembly via the loading port (Figure 1). The assembly was kept still under the fume hood for 30 min at room temperature to achieve full polymerization.

To remove the gel from the mold, first the C-clamps were removed. Then, the top and bottom mold pieces were carefully separated using a gel releaser (BIO-RAD, #165330) on the lateral protrusions, followed by carefully moving the releaser around the internal face of the top. After splitting the top and bottom pieces, the gel was removed by inverting the mold so that the gel is facing thick blotter paper (BIO-RAD #1703958) that is presoaked in running buffer (see below). The blotter paper was approximately 5 cm larger than the gel on the top and bottom and about 1 cm larger than the gel on each side. The gel is slowly peeled away from a corner using the gel releaser until gravity facilitates the remaining gel to gently fall onto the soaked blotter paper support. The gel can be used immediately or be stored in a sealed bag at 4 °C for several months (at least).

Cell Culture. MCF10A cells (from LINCS Consortium and STR verified internally) were cultured in DMEM/F12 (Gibco #11330032) medium containing 5% (v/v) of horse serum (Gibco #16050122), 20 ng/mL of EGF (PeproTech #AF-100-15), 0.5 mg/mL of hydrocortisone (Sigma-Aldrich #H-0888), 10 μg/mL of insulin (Sigma-Aldrich #I-1882), 100 ng/mL of cholera toxin (Sigma-Aldrich #C-8052), and 2 mM of L-glutamine (Corning #25-005-CI). U87 cells (from ATCC and STR verified internally) were cultured in DMEM

https://doi.org/10.1021/acsomega.2c02201
ACS Omega 2022, 7, 28912−28923

(Gibco#10313021) medium containing 10% (v/v) fetal bovine serum (Corning#35-011-CV) and L-glutamine (2 mM) (Corning #25-005-CI). The cells are kept at 37 °C in 5% CO_2 in a humidified incubator. To maintain subconfluency, the cells are passaged every 2−3 days, washing once with phosphate-buffered saline (PBS), lifting with 0.25% trypsin (Corning #25-053-CI), and reseeding in full growth media.

Lysate and Sample Preparation. Cells growing in full growth media were collected, counted, and seeded (150,000 cells/well) in tissue culture-treated 6-well plates (Corning # 08-772-1B). The cells were kept at 37 °C in 5% CO_2 in a humidified incubator for ∼48 h. The plates were removed from the incubator, and media in the wells was aspirated. The wells were washed with ice-cold PBS once and placed on ice. Freshly prepared, ice-cold RIPA buffer (110 μL, 50 mM tris, pH 7−8 (Acros Organics #14050-0010), 150 mM NaCl (Fluka #71383), 0.1% SDS (v/v from 10% stock, Fisher #46040CI), 0.5% sodium deoxycholate (g/mL Alfa Aesar, J62288), 1% Triton-X-100 (v/v, Fisher, BP151) with protease and phosphatase inhibitors (1 μg/mL aprotinin (MP Biomedicals #0219115801), 1 μg/mL leupeptin (MP Biochemicals #0215155301), 1 μg/mL pepstatin A (MP Biochemicals #0219536801), 10 mM β-glycerophosphate (Santa Cruz Biotechnology #sc203323), and 1 mM sodium orthovanadate (Sigma-Aldrich # S6508)) were added into each well. The plates were kept on a rocker (slow) in the cold room for 15 min. Then, the lysates were scraped off with a cell scraper (Stellar Scientific TC-CS-25), and 100 μL lysate from each well was transferred into labeled Eppendorf tubes on ice. Each tube was vortexed three times for ∼30 s to homogenize cell debris. Next, the tubes were centrifuged at 4 °C for 15 min at ∼21,000*g* (max speed). Finally, 80 μL of the supernatant from each tube was transferred into a new Eppendorf tube, being careful not to disturb the debris pellet. Lysates were stored at −20 °C for short-term storage and transferred to −80 °C for long-term storage.

Protein Quantification. Total protein quantification of lysates was done using either the BCA-Pierce 660 Assay (Thermo Scientific #23225) or Pierce Rapid Gold BCA (Thermo Scientific A53225), and BSA stock (Thermo Scientific #23209) was used as a reference according to the manufacturer's protocol. In short, 10 μL of the lysate sample or BSA standards were loaded into 96-well plates (Corning #3370), in triplicate. Then, the BCA Protein Assay Reagent was loaded into each nonempty well. The plate was covered with the lid and incubated at room temperature for 5 min. The absorbance readings at 660 or 480 nm were obtained in a plate reader (BioTek #Epoch2). The average of blank wells was subtracted from each reading to calculate blank-corrected averages for each condition. The standard curve is fitted to a line using blank-corrected mean values of each standard condition versus its BSA concentration. The protein concentration in each sample was calculated using the standard curve formula.

Sample Preparation. Lysate stocks are thawed on ice (if applicable). Then, a 5× sample buffer was prepared (5 mL of glycerol (Sigma-Aldrich #G5516), 0.5 mL of 10% SDS (Fisher #BP 2436), 0.01 g of bromophenol blue (Calbiochem #2830), 2.1 mL of 5× tris-acetate buffer (as above), 0.5 mL of β-mercaptoethanol (Sigma-Aldrich #M6250), then the total volume brought to 10 mL with MilliQ water). This was mixed with lysates in a 1:4 (v/v) ratio. Next, the tubes were heated at 95 °C for 5 min in a dry heating block and then briefly spun in benchtop microcentrifuge before loading (below).

Loading the Gel. Following the release of the gel onto the soaked blotter paper, the assembly was placed down on a flat surface with the wells facing up. If folds and stretching of the gel are evident, light rolling was used to flatten. A p2 micropipette with 10 μL tips was used to load the prepared lysates and/or molecular weight ladder (LI-COR, 928-60000) into wells as desired. We have found that wells less than 2 mm away from the gel boundaries may be subject to inconsistent electrophoresis and transfer and therefore avoid them when possible. Care was taken not to adjust the gel on the blotter paper after any loading and also to transport the gel with a spatula support underneath.

Horizontal Electrophoresis. Horizontal electrophoresis was carried out using the Flatbed Professional (Gel Company Store, FC-EDCProf-2836). The apparatus was maintained at 10 °C during electrophoresis. First, ∼10 mL of cooled running buffer was poured onto the center of the apparatus, followed by transfer of the blotter paper/loaded gel by spatula onto this buffer. Running buffer was made by combining 20 mL of 5× tris-acetate buffer (see above) with 29.5 mL of MilliQ water and 0.5 mL of 10% SDS. The gel should be oriented to have the red bar at the bottom, where the proteins will migrate toward. Additionally, the wells should be aligned with the apparatus gridlines, and excess running buffer should be wiped up with no buffer accumulated outside of the blotter paper. Then, the anode and cathode wires were placed over the blotter paper, about 3 cm from the gel. Finally, the glass plate was placed on top of the anode and cathode and the lid was closed. Electrophoresis was conducted at 100 V for ∼2 h, although each run should be individually monitored. Samples should be visible as blue dots in the gel after ∼30 min, and ideally, the run should be stopped when it reaches the top edge of the next well. After 30 min, we paused the run, lifted the blotter paper and gel with a spatula, and rehydrated by placing another 10 mL of cool running buffer as previously.

Transfer to Membrane. Transfer buffer was prepared by first making 10× tris-glycine buffer (600 mL of MilliQ water with 30.3 g of tris base (BIO-RAD #161-0719) and 144 g of glycine (VWR #0167), then MilliQ water was added to a final volume of 800 mL). Transfer buffer (∼2 L, 1×) was made by taking 160 mL of 10× tris-glycine buffer, adding MilliQ water up to a final volume of 1600 mL, and finally, adding ∼400 mL of methanol (Fisher #A412-in a fume hood) to 2 L. Transfer buffer is stored at 4 °C.

For quarter gels, we used a Mini Trans-Blot Cell (BIO-RAD, 1703930), and for full gels, we used a Criterion Blotter (BIO-RAD, 1704070). We have successfully used both nitrocellulose (GE, 10600002) and PVDF (BIO-RAD, 1620264) membranes for Mesowestern, and in this work, the data come from PVDF. In our experience, low fluorescence PVDF membranes tend to provide a better signal to noise due to their increased ability to bind low abundance proteins, although answering such questions definitively was not the purpose of this manuscript. For PVDF, the membrane was prewet with methanol prior to subsequent use and never allowed to dry out.

To prepare the gel and membrane for transfer, cold transfer buffer was poured into a pyrex dish to a depth of ∼3 cm. Blotter paper, cut to the size of the transfer cassette but larger than the gel, was placed into the pyrex dish to soak. After soaking, the blotter paper was placed on a clean, flat benchtop. Then, the gel was allowed to soak in the same transfer buffer

https://doi.org/10.1021/acsomega.2c02201
ACS Omega 2022, 7, 28912−28923

for ∼15 min, making sure to keep track of which side of the gel has the well indentations. The gel was then placed onto the soaked blotter paper, with the wells facing down on the paper. A spatula was always used to transport the gel. The gel was then gently rolled flat, and air pockets were removed using a roller (BIO-RAD, 1651279). The membrane was cut to the same size as the gel, being careful never to touch the membrane except with clean tools. After wetting with methanol (if PVDF is used), the membrane was then placed to soak in transfer buffer. Forceps were used to gently place the membrane onto the gel. If the membrane is not aligned, we did not move it, rather, we got a new membrane. Then, the membrane was rolled as previously. A second piece of transfer buffer-soaked blotter paper was then placed on top of the membrane in line with the first piece of blotter paper and rolled as previously. Finally, a spatula was used to lift the "sandwich" onto a fiber pad (BIO-RAD, 1703933), and another fiber pad was placed on top. This fiber pad-surrounded sandwich was moved to the transfer cassette, making sure that the side of the sandwich closest to the membrane was on the clear/positive side of the cassette (BIO-RAD, 1703931). This also means that the side of the sandwich closest to the gel is on the black/negative side of the cassette. The cassette was then placed into the transfer apparatus (negative to negative/black to black, positive to positive/clear to red). If desired, a second sandwich was made and placed into the apparatus.

With the cassettes in the transfer apparatus, a cold transfer buffer was added until it reached the indicated volume line. The apparatus was moved to a 4 °C room, and then transfer was carried out at 30 V for 16 h (usually overnight). After the transfer, the membrane was removed with clean forceps and was placed in a clean incubation box (Li-Cor, 929-97201), with the side of the membrane that was in contact with the gel facing up.

Antibody Incubation. First, TBS and TBST buffers were prepared. Briefly, 10× TBS was made by dissolving a 24 g tris base (BIO-RAD #161-0719) and 88 g NaCl (CAS 7647-14-5) in 1 L of MilliQ water. The pH was monitored with continuous magnetic stirring while adding HCl dropwise to bring the pH to 7.6. To make 1× TBS, 50 mL of 10× TBS was added to 450 mL of MilliQ water and stored at 4 °C (stable for several months). To make 1× TBST, 2.5 mL of 10% Tween 20 (BIO-RAD #161-0781) was added to 500 mL of 1× TBS and similarly stored at 4 °C.

All membrane incubations were done in the dark (sealed black box or covered in aluminum foil). The membrane was incubated first in ∼20 mL of blocking buffer (1 g BSA (Fisher, BP1600) in 20 mL of 1× TBS) for at least 30 min at room temperature with gentle rocking. After blocking, the blocking buffer was removed, and the membrane was directly incubated with a primary antibody solution (10 mL blocking buffer, 50 μL of 10% Tween 20, v/v dilution of primary antibody to the desired working concentration) for at least 2 h at room temperature or overnight at 4 °C, all with gentle rocking. After primary antibody incubation, the membrane was washed with ∼10 mL of 1× TBST three times, 5 min for nitrocellulose, and four times, 15 min for PVDF. After washing, the secondary antibody solution (10 mL 1× TBST with 1:20,000 v/v; see below) was added to the membrane and incubated with gentle rocking for 1 h at room temperature. After incubation, the secondary antibody solution was discarded, and the membrane was washed as previously with 1× TBST. After the last TBST wash, a final TBS wash was done. The membrane was then scanned with the side that was facing up (closest to gel during transfer) now facing down on the clean surface of a LI-COR Odyssey infrared fluorescence scanning instrument (LI-COR model number 9140).

Antibodies were obtained from and used with working concentrations as follows: p-MAPK (Cell Signaling, #4370S, 1:1000), α-tubulin (Novus, #NB100-690, 1:1000), β-actin (Figure 5: LI-COR #926-42212, 1:1000; Figure 7: Cell Signaling, #3700, 1:1000), antirabbit (800CW LI-COR #926-32211, 1:20,000), and antimouse (680LT LI-COR #925-68070, 1:20,000).

Imaging and Quantification. Placement of the membrane on the scanning surface was set in Image Studio. Both 700 nm and 800 nm wavelength channels were set to be scanned. Resolution was set to generally 42 μm (some exceptions for speed at times), and the focus offset was set to 0.0 mm. After the membrane finished scanning, the image and the associated zip file were exported from the Li-Cor Odyssey scanner and imported into Image Studio Lite for analysis. In Image Studio, boxes were drawn around protein bands and the "signal" metric generated by the software was used as the quantification.[7,37]

■ ASSOCIATED CONTENT

Supporting Information

The Supporting Information is available free of charge at https://pubs.acs.org/doi/10.1021/acsomega.2c02201.

Full scans of the results shown in Figure 4 of the main text (Figure S1) and full scans of the results shown in Figure 7 of the main text (Figure S2) (PDF)

■ AUTHOR INFORMATION

Corresponding Author

Marc R. Birtwistle − *Department of Chemical and Biomolecular Engineering, Clemson University, Clemson, South Carolina 29634, United States; Department of Bioengineering, Clemson University, Clemson, South Carolina 29634, United States;* orcid.org/0000-0002-0341-0705; Email: mbirtwi@clemson.edu

Authors

Cameron O. Zadeh − *Department of Chemical and Biomolecular Engineering, Clemson University, Clemson, South Carolina 29634, United States*

Jonah R. Huggins − *Department of Chemical and Biomolecular Engineering, Clemson University, Clemson, South Carolina 29634, United States;* orcid.org/0000-0001-7468-4626

Deepraj Sarmah − *Department of Chemical and Biomolecular Engineering, Clemson University, Clemson, South Carolina 29634, United States*

Baylee C. Westbury − *Department of Chemical and Biomolecular Engineering, Clemson University, Clemson, South Carolina 29634, United States*

William R. Interiano − *Department of Chemical and Biomolecular Engineering, Clemson University, Clemson, South Carolina 29634, United States*

Micah C. Jordan − *Department of Chemical and Biomolecular Engineering, Clemson University, Clemson, South Carolina 29634, United States*

https://doi.org/10.1021/acsomega.2c02201
ACS Omega 2022, 7, 28912−28923

S. Ashley Phillips − *Department of Chemical and Biomolecular Engineering, Clemson University, Clemson, South Carolina 29634, United States*
William B. Dodd − *Department of Chemical and Biomolecular Engineering, Clemson University, Clemson, South Carolina 29634, United States*
Wesley O. Meredith − *Department of Chemical and Biomolecular Engineering, Clemson University, Clemson, South Carolina 29634, United States*
Nicholas J. Harold − *Department of Chemical and Biomolecular Engineering, Clemson University, Clemson, South Carolina 29634, United States*
Cemal Erdem − *Department of Chemical and Biomolecular Engineering, Clemson University, Clemson, South Carolina 29634, United States;* orcid.org/0000-0003-3663-3646

Complete contact information is available at: https://pubs.acs.org/10.1021/acsomega.2c02201

Author Contributions

§C.O.Z. and J.R.H. contributed equally.

Notes

The authors declare the following competing financial interest(s): Authors Dr. Marc Birtwistle, Cameron Zadeh, and Jonah Huggins are co-founders of Blotting Innovations LLC.

■ ACKNOWLEDGMENTS

Funding for this project was, in part, provided by the NIH/NHGRI grant U54HG008098, NIH/NIGMS R35GM141891, and by Clemson University. The authors thank Tim Pruett in the Clemson Additive Manufacturing core for 3D printing services and Mark Ciaccio for helpful discussions.

■ REFERENCES

(1) Towbin, H.; Staehelin, T.; Gordon, J. Electrophoretic Transfer of Proteins from Polyacrylamide Gels to Nitrocellulose Sheets: Procedure and Some Applications. *Proc. Natl. Acad. Sci. U.S.A.* **1979**, *76*, 4350−4354.
(2) Hnasko, T. S.; Hnasko, R. M.The Western Blot. In *Methods in Molecular Biology*; Humana Press: New York, NY, 2015; Vol. *1318*, pp 87−96. DOI: DOI: 10.1007/978-1-4939-2742-5_9.
(3) Kurien, B. T.; Scofield, R. H.Western Blotting: An Introduction. In *Methods in Molecular Biology*; Humana Press: New York, NY, 2015; Vol. *1312*, pp 17−30. DOI: DOI: 10.1007/978-1-4939-2694-7_5.
(4) *Protein Blotting and Detection* Kurien, B. T.; Scofield, R. H., Eds.; Humana Press: Totowa, NJ, 2009; Vol. *536* DOI: 10.1007/978-1-59745-542-8.
(5) Alegria-Schaffer, A.; Lodge, A.; Vattem, K. Chapter 33 Performing and Optimizing Western Blots with an Emphasis on Chemiluminescent Detection. In *Methods Enzymology*, Elsevier, 2009; Vol. *463*, pp 573−599. DOI: DOI: 10.1016/S0076-6879(09)63033-0.
(6) Mathews, S. T.; Plaisance, E. P.; Kim, T. Imaging Systems for Westerns: Chemiluminescence vs. Infrared Detection. In *Protein Blotting and Detection*, Kurien, B. T.; Scofield, R. H., Eds.; Humana Press: Totowa, NJ, 2009; Vol. *536*, pp 499−513. DOI: DOI: 10.1007/978-1-59745-542-8_51.
(7) Janes, K. A. An Analysis of Critical Factors for Quantitative Immunoblotting. *Sci. Signal.* **2015**, *8*, rs2.
(8) Degasperi, A.; Birtwistle, M. R.; Volinsky, N.; Rauch, J.; Kolch, W.; Kholodenko, B. N. Evaluating Strategies to Normalise Biological Replicates of Western Blot Data. *PLoS One* **2014**, *9*, No. e87293.
(9) Pillai-Kastoori, L.; Schutz-Geschwender, A. R.; Harford, J. A. A Systematic Approach to Quantitative Western Blot Analysis. *Anal. Biochem.* **2020**, *593*, No. 113608.
(10) Moritz, C. P. 40 Years Western Blotting: A Scientific Birthday Toast. *J. Proteomics* **2020**, *212*, No. 103575.
(11) Uhlen, M.; Bandrowski, A.; Carr, S.; Edwards, A.; Ellenberg, J.; Lundberg, E.; Rimm, D. L.; Rodriguez, H.; Hiltke, T.; Snyder, M.; Yamamoto, T. A Proposal for Validation of Antibodies. *Nat. Methods* **2016**, *13*, 823−827.
(12) Baker, M. Reproducibility Crisis: Blame It on the Antibodies. *Nature* **2015**, *521*, 274−276.
(13) Krajewski, S.; Tsukamoto, M. M.; Huang, X.; Krajewski, S. B. Nonstripping "Rainbow" and Multiple Antigen Detection (MAD) Western Blotting. In *Detection of Blotted Proteins* Kurien, B. T.; Scofield, R. H., Eds.; Methods in Molecular Biology; Springer New York: New York, NY, 2015; Vol. *1314*, pp 287−301. DOI: DOI: 10.1007/978-1-4939-2718-0_30.
(14) Aksamitiene, E.; Hoek, J. B.; Kholodenko, B.; Kiyatkin, A. Multistrip Western Blotting to Increase Quantitative Data Output. *ELECTROPHORESIS* **2007**, *28*, 3163−3173.
(15) Aksamitiene, E.; Hoek, J. B.; Kiyatkin, A. Multistrip Western Blotting: A Tool for Comparative Quantitative Analysis of Multiple Proteins. In *Western Blotting*; Kurien, B. T.; Scofield, R. H., Eds.; Methods in Molecular Biology; Springer New York: New York, NY, 2015; Vol. *1312*, pp 197−226. DOI: DOI: 10.1007/978-1-4939-2694-7_23.
(16) Krajewski, S.; Huang, X.; Krajewska, M. Multiple Antigen Detection (MAD) Western Blotting. In *Protein Blotting and Detection* Kurien, B. T.; Scofield, R. H., Eds.; Methods in Molecular Biology; Humana Press: Totowa, NJ, 2009; Vol. *536*, pp 473−481. DOI: DOI: 10.1007/978-1-59745-542-8_48.
(17) Krajewski, S. "Rainbow" Western Blotting. In *Protein Blotting and Detection*; Kurien, B. T.; Scofield, R. H., Eds.; Methods in Molecular Biology; Humana Press: Totowa, NJ, 2009; Vol. *536*, pp 463−472. DOI: DOI: 10.1007/978-1-59745-542-8_47.
(18) Tibes, R.; Qiu, Y.; Lu, Y.; Hennessy, B.; Andreeff, M.; Mills, G. B.; Kornblau, S. M. Reverse Phase Protein Array: Validation of a Novel Proteomic Technology and Utility for Analysis of Primary Leukemia Specimens and Hematopoietic Stem Cells. *Mol. Cancer Ther.* **2006**, *5*, 2512−2521.
(19) Hennessy, B. T.; Lu, Y.; Gonzalez-Angulo, A. M.; Carey, M. S.; Myhre, S.; Ju, Z.; Davies, M. A.; Liu, W.; Coombes, K.; Meric-Bernstam, F.; Bedrosian, I.; McGahren, M.; Agarwal, R.; Zhang, F.; Overgaard, J.; Alsner, J.; Neve, R. M.; Kuo, W.-L.; Gray, J. W.; Borresen-Dale, A.-L.; Mills, G. B. A Technical Assessment of the Utility of Reverse Phase Protein Arrays for the Study of the Functional Proteome in Non-Microdissected Human Breast Cancers. *Clin. Proteomics* **2010**, *6*, 129−151.
(20) Earley, M. C.; Vogt, R. F.; Shapiro, H. M.; Mandy, F. F.; Kellar, K. L.; Bellisario, R.; Pass, K. A.; Marti, G. E.; Stewart, C. C.; Hannon, W. H. Report from a Workshop on Multianalyte Microsphere Assays. *Cytometry* **2002**, *50*, 239−242.
(21) He, J. Practical Guide to ELISA Development. In *The Immunoassay Handbook*, Elsevier, 2013; pp 381−393. DOI: DOI: 10.1016/B978-0-08-097037-0.00025-7.
(22) Engvall, E.; Perlmann, P. Enzyme-Linked Immunosorbent Assay, Elisa. 3. Quantitation of Specific Antibodies by Enzyme-Labeled Anti-Immunoglobulin in Antigen-Coated Tubes. *J. Immunol.* **1972**, *109*, 129−135.
(23) Aebersold, R.; Mann, M. Mass-Spectrometric Exploration of Proteome Structure and Function. *Nature* **2016**, *537*, 347−355.
(24) Wilhelm, M.; Schlegl, J.; Hahne, H.; Moghaddas Gholami, A.; Lieberenz, M.; Savitski, M. M.; Ziegler, E.; Butzmann, L.; Gessulat, S.; Marx, H.; Mathieson, T.; Lemeer, S.; Schnatbaum, K.; Reimer, U.; Wenschuh, H.; Mollenhauer, M.; Slotta-Huspenina, J.; Boese, J.-H.; Bantscheff, M.; Gerstmair, A.; Faerber, F.; Kuster, B.; Gholami, A. M.; Lieberenz, M.; Savitski, M. M.; Ziegler, E.; Butzmann, L.; Gessulat, S.; Marx, H.; Mathieson, T.; Lemeer, S.; Schnatbaum, K.; Reimer, U.; Wenschuh, H.; Mollenhauer, M.; Slotta-Huspenina, J.; Boese, J.-H.; Bantscheff, M.; Gerstmair, A.; Faerber, F.; Kuster, B. Mass-Spectrometry-Based Draft of the Human Proteome. *Nature* **2014**, *509*, 582−587.

(25) Shevchenko, A.; Tomas, H.; Havlis, J.; Olsen, J. V.; Mann, M. In-Gel Digestion for Mass Spectrometric Characterization of Proteins and Proteomes. *Nat. Protoc.* **2006**, *1*, 2856−2860.
(26) Bittremieux, W.; Tabb, D. L.; Impens, F.; Staes, A.; Timmerman, E.; Martens, L.; Laukens, K. Quality Control in Mass Spectrometry-Based Proteomics. *Mass Spectrom. Rev.* **2018**, *37*, 697−711.
(27) Yates, J. R.; Ruse, C. I.; Nakorchevsky, A. Proteomics by Mass Spectrometry: Approaches, Advances, and Applications. *Annu. Rev. Biomed. Eng.* **2009**, *11*, 49−79.
(28) Handler, D. C.; Pascovici, D.; Mirzaei, M.; Gupta, V.; Salekdeh, G. H.; Haynes, P. A. The Art of Validating Quantitative Proteomics Data. *PROTEOMICS* **2018**, *18*, No. 1800222.
(29) Hughes, A. J.; Spelke, D. P.; Xu, Z.; Kang, C.-C.; Schaffer, D. V.; Herr, A. E. Single-Cell Western Blotting. *Nat. Methods* **2014**, *11*, 749−755.
(30) Kang, C.-C.; Yamauchi, K. A.; Vlassakis, J.; Sinkala, E.; Duncombe, T. A.; Herr, A. E. Single Cell-Resolution Western Blotting. *Nat. Protoc.* **2016**, *11*, 1508−1530.
(31) Sanders, B. J.; Kim, D. C.; Dunn, R. C. Recent Advances in Microscale Western Blotting. *Anal. Methods* **2016**, *8*, 7002−7013.
(32) O'Neill, R. A.; Bhamidipati, A.; Bi, X.; Deb-Basu, D.; Cahill, L.; Ferrante, J.; Gentalen, E.; Glazer, M.; Gossett, J.; Hacker, K.; Kirby, C.; Knittle, J.; Loder, R.; Mastroieni, C.; MacLaren, M.; Mills, T.; Nguyen, U.; Parker, N.; Rice, A.; Roach, D.; Suich, D.; Voehringer, D.; Voss, K.; Yang, J.; Yang, T.; Vander Horn, P. B. Isoelectric Focusing Technology Quantifies Protein Signaling in 25 Cells. *Proc. Natl. Acad. Sci. U.S.A.* **2006**, *103*, 16153−16158.
(33) Dengler-Crish, C. M.; Smith, M. A.; Wilson, G. N. Early Evidence of Low Bone Density and Decreased Serotonergic Synthesis in the Dorsal Raphe of a Tauopathy Model of Alzheimer's Disease. *J. Alzheimers Dis.* **2016**, *55*, 1605−1619.
(34) Treindl, F.; Ruprecht, B.; Beiter, Y.; Schultz, S.; Döttinger, A.; Staebler, A.; Joos, T. O.; Kling, S.; Poetz, O.; Fehm, T.; Neubauer, H.; Kuster, B.; Templin, M. F. A Bead-Based Western for High-Throughput Cellular Signal Transduction Analyses. *Nat. Commun.* **2016**, *7*, No. 12852.
(35) Ciaccio, M. F.; Jones, R. B. Microwestern Arrays for Systems-Level Analysis of SH2 Domain-Containing Proteins. *Methods Mol. Biol.* **2017**, 453−473.
(36) Ciaccio, M. F.; Wagner, J. P.; Chuu, C.-P.; Lauffenburger, D. A.; Jones, R. B. Systems Analysis of EGF Receptor Signaling Dynamics with Microwestern Arrays. *Nat. Methods* **2010**, *7*, 148−155.
(37) Koch, R. J.; Barrette, A. M.; Stern, A. D.; Hu, B.; Bouhaddou, M.; Azeloglu, E. U.; Iyengar, R.; Birtwistle, M. R. Validating Antibodies for Quantitative Western Blot Measurements with Microwestern Array. *Sci. Rep.* **2018**, *8*, No. 11329.
(38) Stacking Gel (5%). *Cold Spring Harb. Protoc.* 2006, *2006* (5), pdb.rec10666. DOI: DOI: 10.1101/pdb.rec10666.
(39) Walker, J. M. Gradient SDS Polyacrylamide Gel Electrophoresis. In *Proteins*; Humana Press: New Jersey, 1984; Vol. *1*, pp 57−62. DOI: 10.1385/0-89603-062-8:57.
(40) Wiśniewski, J. R.; Hein, M. Y.; Cox, J.; Mann, M. A "Proteomic Ruler" for Protein Copy Number and Concentration Estimation without Spike-in Standards. *Mol. Cell. Proteomics* **2014**, *13*, 3497−3506.
(41) Macromolecular Components of E. coli and HeLa Cells - US. www.thermofisher.com/us/en/home/references/ambion-tech-support/rna-tools-and-calculators/macromolecular-components-of-e.html (accessed 2022-04-06).
(42) HeLa cell volume - Human Homo sapiens - BNID 103725. https://bionumbers.hms.harvard.edu/bionumber.aspx?id=103725&ver=14 (accessed 2022-04-06).
(43) Fan, B.; Li, X.; Liu, L.; Chen, D.; Cao, S.; Men, D.; Wang, J.; Chen, J. Absolute Copy Numbers of β-Actin Proteins Collected from 10,000 Single Cells. *Micromachines* **2018**, *9*, 254.
(44) Schutz-Geschwender, A.; Zhang, Y.; Holt, T.; McDermitt, D.; Olive, D. M. *Quantitative, Two-Color Western Blot Detection With Infrared Fluorescence*; LI-COR Biosciences, pp 1−8.
(45) Detection Methods. Bio-Rad Laboratories. https://www.bio-rad.com/en-us/applications-technologies/detection-methods?ID=LUSQ6KKG4.
(46) Chrambach, A.; Rodbard, D. Polyacrylamide Gel Electrophoresis. *Science* **1971**, *172*, 440−451.

https://doi.org/10.1021/acsomega.2c02201
ACS Omega 2022, 7, 28912−28923